ORNL-TM-4495

AUGER ELECTRON SPECTROSCOPY OF FRACTURE SURFACES IN IRRADIATED TYPE 304 STAINLESS STEEL

E. E. Bloom
R. E. Clausing

OAK RIDGE NATIONAL LABORATORY
OPERATED BY UNION CARBIDE CORPORATION • FOR THE U.S. ATOMIC ENERGY COMMISSION

ORNL-TM-4495

Contract No. W-7405-eng-26

METALS AND CERAMICS DIVISION

AUGER ELECTRON SPECTROSCOPY OF FRACTURE SURFACES IN IRRADIATED TYPE 304 STAINLESS STEEL

E. E. Bloom and R. E. Clausing

MARCH 1974

OAK RIDGE NATIONAL LABORATORY
Oak Ridge, Tennessee 37830
operated by
UNION CARBIDE CORPORATION
for the
U.S. ATOMIC ENERGY COMMISSION

CONTENTS

AUGER ELECTRON SPECTROSCOPY OF FRACTURE SURFACES IN IRRADIATED TYPE 304 STAINLESS STEEL

E. E. Bloom and R. E. Clausing

ABSTRACT

Auger electron spectroscopy has been used to study surfaces in type 304 stainless steel fractured after irradiation at 370°C to 1.4–10 × 10^{22} neutrons/cm^2. At the temperatures and strain rates employed, the irradiated samples failed primarily along grain boundaries, although in some cases areas of ductile transgranular fracture were also present. Helium release during fracture was monitored with a residual gas analyzer. The concentration of helium at the boundaries was approximately proportional to the fast neutron fluence to which the samples were irradiated, being about 0.08 helium atoms per grain boundary site at 1 × 10^{23} neutrons/cm^2. Phosphorus was more concentrated at grain boundaries than on ductile fracture surfaces. Sulfur segregated to surfaces during and after the fracture, making the analysis for the element somewhat less conclusive. The fact that it segregated to surfaces, however, suggests that it could segregate to grain boundaries. Grain boundary fracture surfaces of irradiated samples were depleted in chromium and enriched in iron and nickel compared with ductile fractures of unirradiated samples broken at the same temperature.

INTRODUCTION

The reduction in elevated-temperature ductility of austenitic stainless steels due to neutron irradiation depends on the irradiation and postirradiation test conditions.[1-5] For irradiation temperatures and

---

[1]E. E. Bloom, "Correlation of Structure and Ductility of Irradiated Austenitic Stainless Steels," paper presented at BNES Conference on Irradiation Embrittlement and Creep in Fuel Cladding and Core Components, Nov. 9–10, 1972, London. To be published in Proceedings.

[2]E. E. Bloom and J. O. Stiegler, "Effect of Irradiation on the Microstructure and Creep-Rupture Properties of Type 316 Stainless Steel," paper presented at ASTM Symposium on Effects of Radiation on Structural Materials, Los Angeles, June 25–30, 1972. To be published in Proceedings.

[3]J. Standring et al., "Effects of Neutron Irradiation on Creep-Rupture Properties of Type 316 Stainless Steel Tubes," pp. 414–28 in *Irradiation Effects in Structural Alloys for Thermal and Fast Reactors, Spec. Tech. Publ. 457*, American Society for Testing and Materials, Philadelphia, 1969.

neutron fluences where significant matrix strengthening occurs (i.e., temperatures where voids and a dislocation structure are formed) grain-boundary cracks are initiated during testing and undergo a period of slow stable growth followed by unstable propagation and then fracture when a critical crack size is reached. This behavior can be rationalized, at least in part, on the basis of reduction in the energy required for crack propagation due to the reduced plastic deformation that can occur at the crack tip.[5] This cannot be the complete explanation, however, since the strength of the matrix of an unirradiated sample can be increased by cold working to the same (or even a higher) level as that resulting from the irradiation, yet such cold working by itself does not give rise to the pronounced tendency for intergranular fracture that is observed in material subjected to neutron irradiation. It has been suggested that helium produced by (n,α) transmutations may play a role in the fracture mechanism.[1,2] However, helium bubbles are not generally observed on the grain boundaries for irradiation and test conditions that produce maximum reductions in ductility. Furthermore, the fractures result from enhanced propagation of wedge-type cracks rather than by the simple diffusion-controlled growth and linking of helium bubbles, which suggests that the classical high-temperature embrittlement model of stress-induced bubble growth does not apply to these conditions. It appears that in addition to the effects of matrix strengthening there may be a change in the relative surface and grain boundary energies such that grain boundary fracture becomes more energetically favorable even at temperatures below half the absolute melting temperature.

Changes in grain boundary energy could occur if the composition of the grain boundary region were altered by irradiation. As discussed by Anthony[6] compositional changes occur if the boundary acts as a vacancy sink, in which case substitutional elements with high diffusion coefficient become depleted relative to those with lower diffusion coefficients, or if an element present in the alloy is bound strongly to a defect (vacancy or self-interstitial) that is diffusing to the boundary.

To study the effects of fast-neutron irradiation on the composition of grain boundaries, we modified an Auger electron spectrometer to allow *in situ* fracture of small samples of highly irradiated stainless steel

---

[4]J. J. Holmes, A. J. Lovell, and R. L. Fish, "Ductility Limitations of Irradiated Type 316 Stainless Steel," paper presented at ASTM Symposium on Effects of Radiation on Structural Materials, Los Angeles, June 25–30, 1972. To be published in Proceedings.

[5]M. Weisz et al., "High-Temperature Embrittlement of AISI Type 316 Austenitic Stainless Steels after Irradiation," pp. 352–70 in *Irradiation Effects in Structural Alloys for Thermal and Fast Reactors, Spec. Tech. Publ. 457*, American Society for Testing and Materials, Philadelphia, 1969.

[6]T. R. Anthony, "Solute Segregation and Stresses Generated Around Growing Voids in Metals," pp. 630–46 in *Radiation-Induced Voids in Metals* (Proc. Int. Conf., Albany, N.Y., June 9–11, 1971) ed. by J. W. Corbett and L. C. Ianniello, AEC Symp. Ser. 26, CONF-710601 (April 1972).

at elevated temperatures in vacuum of about 2×10^{-9} torr. At the temperatures and strain rates employed, the irradiated samples failed along the grain boundaries. The composition of the boundaries could thus be examined through analysis of the Auger electron spectrum.

EXPERIMENTAL

The present studies were conducted on samples of type 304 stainless steel that had been machined from a safety rod thimble that had been irradiated in the Experimental Breeder Reactor II (EBR-II). The composition of the thimble material is given in Table 1. The thimble was placed in the reactor in the annealed condition. During irradiation there was a gradient in both irradiation temperature and neutron flux along its length. The inlet and the outlet coolant temperatures were 370 and 460°C, respectively. The peak neutron fluence was 1.7×10^{23} neutrons/cm^2. (All fluence values are for neutrons with energies in excess of 0.1 MeV.) Transmission microscopy, tensile properties, and creep-rupture properties of this material have been reported previously.[7-9] Of importance is the fact that at 450, 550, and 600°C test temperatures, intergranular fractures characteristic of low ductility (0.1–0.2% total creep elongation) were observed.

---

[7]E. E. Bloom, J. O. Stiegler, and C. J. McHargue, "Radiation Damage in Annealed Type 304 Stainless Steel," *Radiat. Eff.* 14: 231–43 (1972).

[8]C. W. Hunter, R. L. Fish, and J. J. Holmes, "Channel Fracture in Irradiated EBR-II Type 304 Stainless Steel," *Trans. Amer. Nucl. Soc.* 15: 254 (1972).

[9]E. E. Bloom, "Creep Properties and Fracture Behavior of Irradiated Type 304 Stainless Steel," to be published.

Table 1. Composition of Unirradiated EBR-II Safety and Control Rod Thimble

Element	Content (wt %)	Element	Content (wt %)
C	0.046	Mo	0.01
Cr	19.0	P	0.012
Ni	9.6	S	0.013
Mn	1.2	B	0.00002
Si	0.6	N	0.004
Ti	<0.05		

Samples for Auger electron spectroscopy were machined from selected positions along the thimble to give the desired combinations of temperature and neutron fluence. The samples were about 1 cm long and 0.1 × 0.1 cm square in cross section, with the center portion of the sample reduced to a 0.05 × 0.05 cm or 0.05 × 0.10 cm cross section to facilitate fracture at the desired position. Figure 1 shows a sample assembled into the two specimen grips of the tensile apparatus. The samples were resistance heated by passing a current from one specimen grip to the other. Sample temperatures were measured either optically or with a small (0.013-cm-diam) thermocouple, which was spot welded to the reduced section of the specimen.

Care was taken to avoid a temperature excursion as the sample resistance changed as a result of crack formation and necking during fracture. To minimize such effects, the heating current was obtained from an alternating-current transformer having a secondary with low inductance, low internal resistance, and good voltage regulation. The output of the transformer was divided between the sample and a noninductive very low-resistance shunt circuit, which carried three to four times the sample current. With this setup, a relatively small change in total

Fig. 1. Specimen, Specimen Holder, and One-Half of Specimen Holder Containing Fractured Specimen for Auger Analysis of Fracture Surface.

power supply voltage occurred when the sample broke. No arcing or increase in sample temperature was detected during visual observation of the sample in a dark room, nor did scanning electron microscopic (SEM) examination of the fracture surfaces reveal any sign of arcing or temperature excursions.

Figure 2 is a schematic drawing of the tensile apparatus. Load was applied to the specimen by adjusting the tension in a spring that was connected by pull rods to the two halves of the specimen holder. When the sample fractured, the circuit was broken and heating stopped. A typical cooling curve went from 550 to 350°C within about a second and to 250°C in 10 min. A mass spectrometer was incorporated into the Auger apparatus to analyze the residual gas remaining in the ultrahigh vacuum. The analyzer was used during the present tests to determine if helium was released as the irradiated samples were strained and/or fractured. Auger electron spectra were taken at various known positions on the fracture surface. The nature of the fracture at these positions was subsequently determined by SEM.

The system used for these analyses includes a Physical Electronics model 12-25G high-resolution cylindrical-mirror electron spectrometer for detecting Auger electrons. The electron beam was typically 2 μA at 300 eV and about 50 to 100 μm in diameter (full width at half maximum). The spectrometer pass energy modulation was 2 eV. Qualitative analysis was accomplished through a comparison of the observed Auger electron spectra

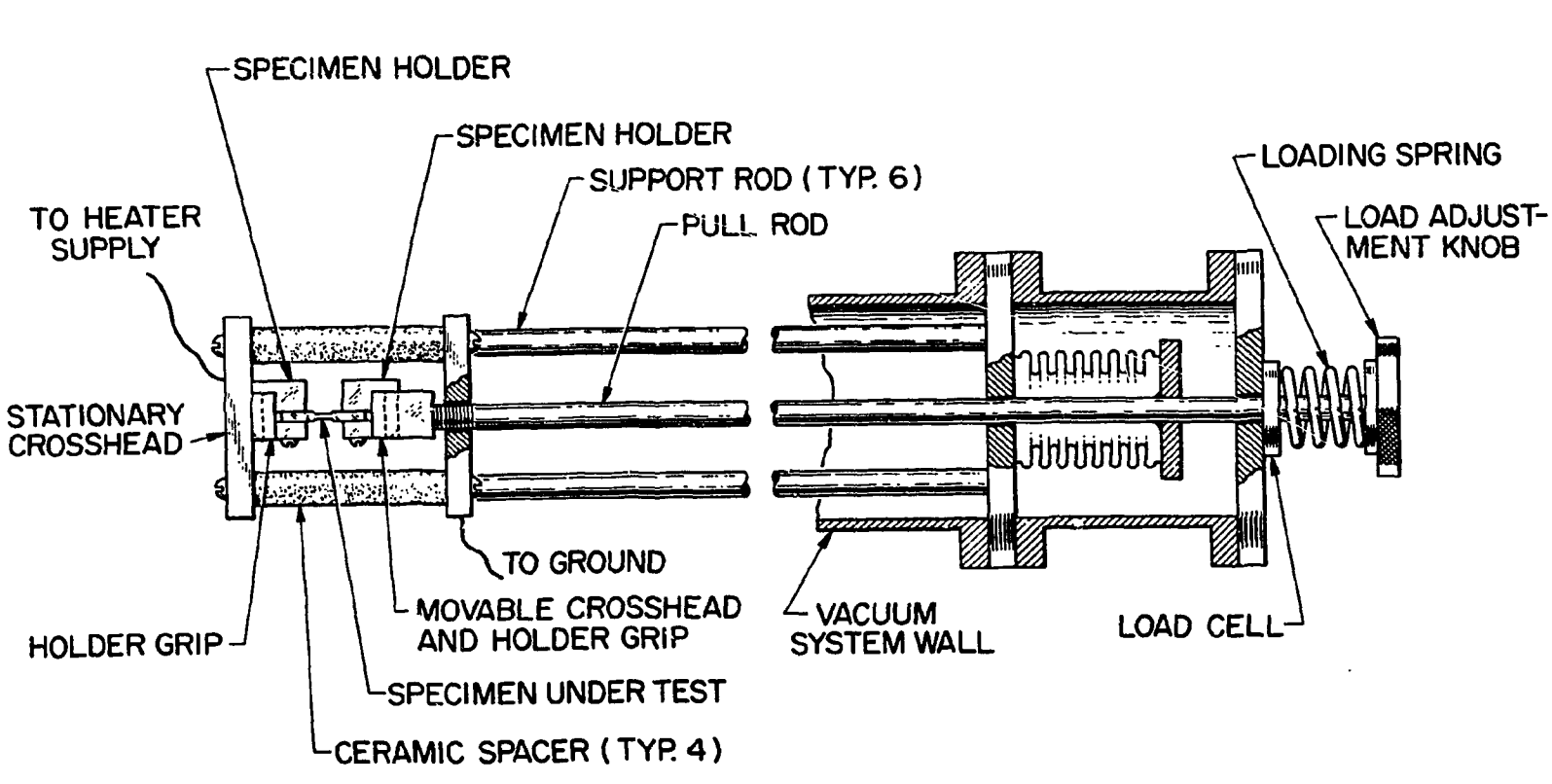

Fig. 2. Schematic Drawing of Tensile Apparatus Contained Within the Vacuum System of the Auger Spectrometer.

[$dN(E)/dE$, as a function of E, where $N(E)$ is the energy distribution function] with the standard[10] Auger spectra. The relative amounts of iron, nickel, and chromium on the fracture surfaces were obtained by measuring the peak-to-peak heights for the Fe_{703}, Ni_{848}, and Cr_{529} lines (the subscript represents the Auger electron energy in eV), adjusting these heights by the relative sensitivity factors[10] of 78, 88, and 105, and then normalizing by setting the sum of these three elements equal to unity. Also, the atomic ratios of P/Fe, S/Fe, etc. were estimated by dividing the observed peak heights by the respective relative sensitivity factors. The first spectra from each sample were obtained within a few minutes after fracture, and pressures were typically 2×10^{-9} torr during the analysis. Most of the residual gases were hydrogen and inert gases, but carbon monoxide was present in amounts large enough to cause a buildup of carbon and oxygen during the analysis and limit the useful carbon and oxygen data to those obtained within the first few minutes after fracture.

The x,y coordinates of each spot were recorded, and the nature of the fracture at that point was determined by SEM examination following completion of the Auger analysis. Composition as a function of depth into the sample was determined by sputtering to remove surface layers. The usual sputtering conditions were argon ions at 1000 eV from a normal-incidence gun. Removal rates were estimated to be one atomic layer per minute.

RESULTS

At all temperatures, the unirradiated samples failed in a ductile-transgranular mode as shown in Fig. 3. Dimples, which were formed by ductile tearing and linking of cavities, and small precipitate particles were the main features observed on the fracture surface. The dimple structure appeared to form on a coarser scale at 550 and 600°C than at 25 and 350°C. Results of Auger analysis of the fracture surfaces of unirradiated samples are summarized in Table 2. The concentration of sulfur on the fracture surface increased with temperature. At 550 and 600°C, small amounts of silicon and phosphorus were also present. With increasing temperature, the concentration of iron decreased and chromium and nickel increased.

Samples irradiated at 370°C to fluences of 1.4×10^{22}, 4.7×10^{22}, and 1×10^{23} neutrons/cm^2 (>0.1 MeV) were fractured at about 550°C and the fracture surfaces analyzed by Auger spectroscopy and then examined by SEM. The fractures of samples irradiated to 1.4×10^{22} and 1×10^{23} neutrons/cm^2 are shown in Figs. 4 and 5, respectively. We believe that the high vacuum and rapid cooling from the test temperature prevented altering the features on these surfaces by oxidation or thermal etching. The sample irradiated to the lower fluence (Fig. 4) failed in

---

[10] P. W. Palmberg et al., *Handbook of Auger Electron Spectroscopy*, Physical Electronics Industries, Inc., Edina, Minn., 1972.

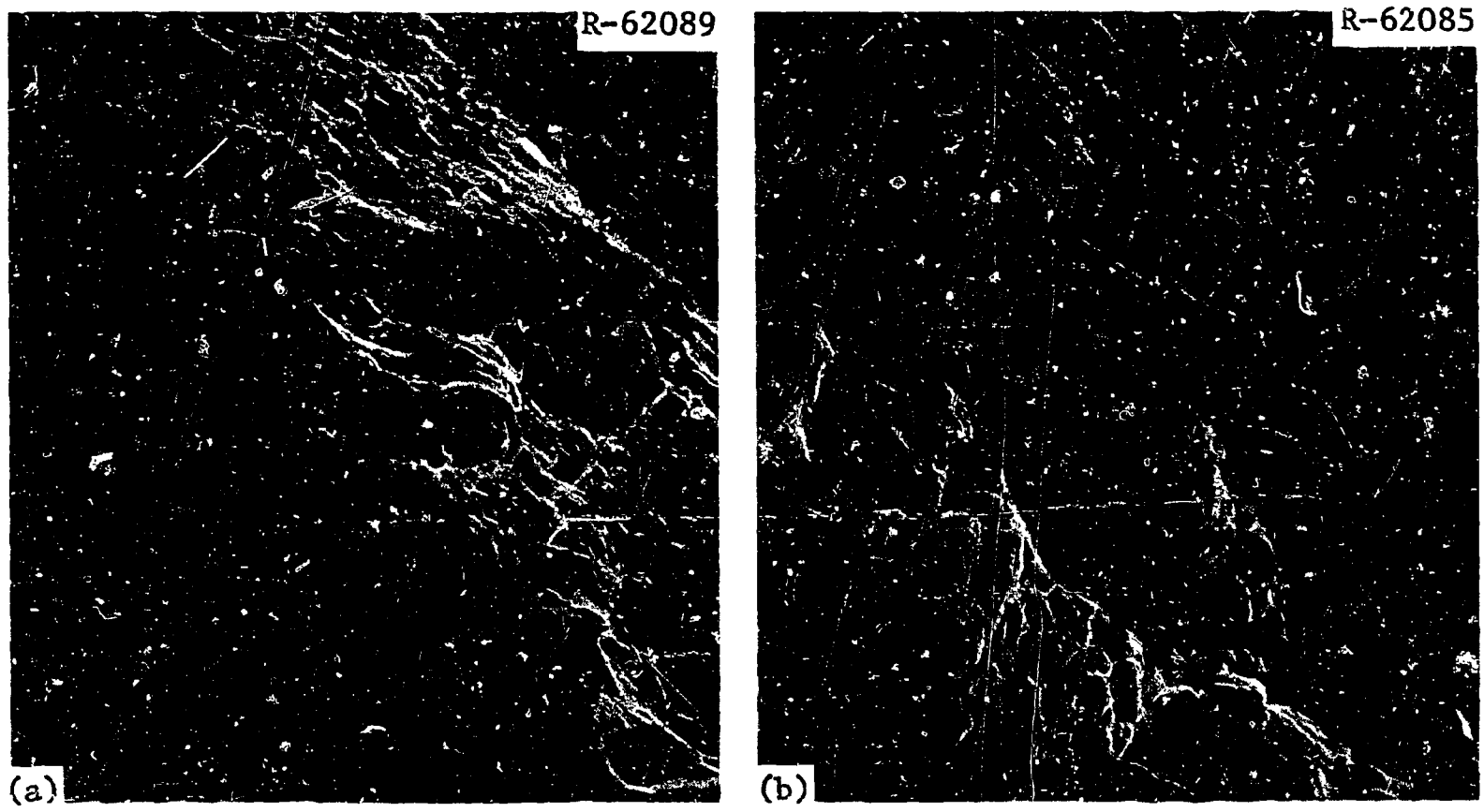

Fig. 3. Fractures of Unirradiated Type 304 Stainless Steel at (a) 450°C and (b) 550°C. 500×.

Table 2. Auger Analyses of the Fracture Surface of Unirradiated Type 304 Stainless Steel as a Function of Test Temperature

Test Temperature (°C)	Atomic Fraction Present, Normalized to Fe + Cr + Ni = 1			Peak Height Ratios			
	Fe	Cr	Ni	Si/Fe	P/Fe	S/Fe	Mn/Fe
25	0.68	0.20	0.12	<0.02	<0.02	0.02	<0.02
350	0.69	0.21	0.10	<0.02	<0.02	0.10	0.12
550	0.60	0.26	0.14	0.03	0.05	0.54	0.11
600	0.59	0.27	0.14	0.04	0.06	0.80	0.22
Cal[a]	0.71	0.19	0.10	0.03	0.00	0.00	0.01

[a]Atomic fractions and peak height ratios based on composition listed in Table 1.

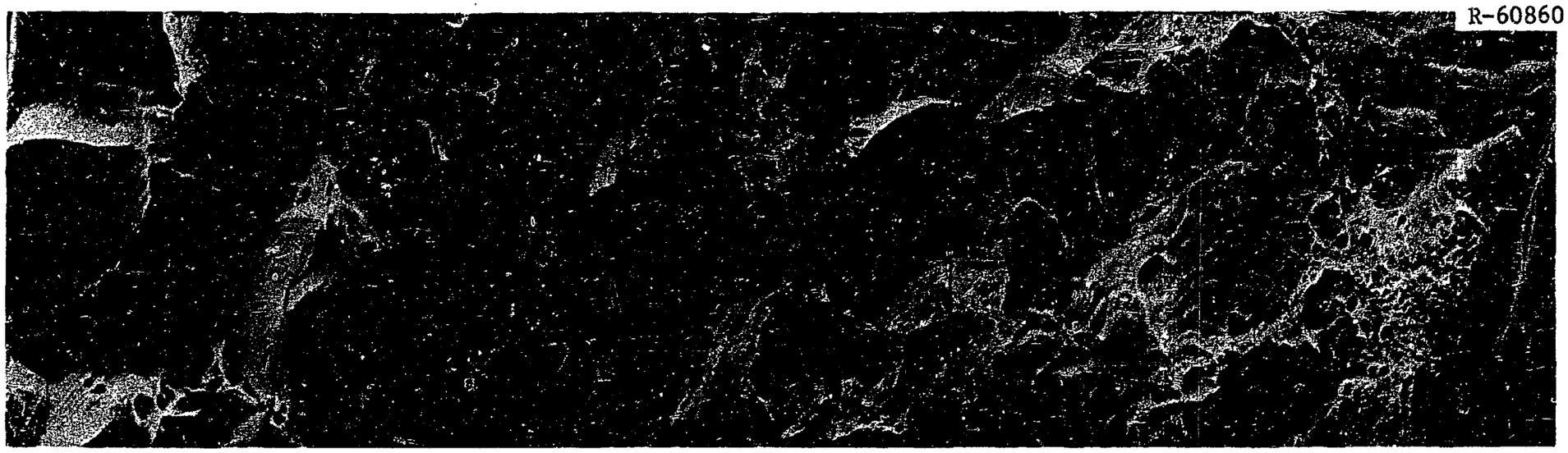

Fig. 4. Fracture Surface of Type 304 Stainless Steel Auger Specimen. The specimen was irradiated to 1.4×10^{22} neutrons/cm^2 (>0.1 MeV) at 370°C and strained to failure at about 550°C in a vacuum of 2×10^{-9} torr. The fracture is mixed intergranular and transgranular. Note the ledges and deformation markings on many of the grain boundary surfaces. 350×. Reduced 9.5%.

Fig. 5. Fracture Surface of Type 304 Stainless Steel Auger Specimen. The specimen was irradiated to 1×10^{23} neutrons/cm^2 (>0.1 MeV) at 374°C and strained to failure at about 550°C in a vacuum of 2×10^{-9} torr. The fracture is in excess of 90% intergranular. 500×. Reduced 13.5%.

a mixed intergranular and transgranular mode. The areas of transgranular fracture are characterized by a dimpled appearance with small precipitate particles often visible in the dimples. On several of the grain boundaries small steps or ledges were present. These are believed to result from the nature of the deformation in the matrix. Instead of occurring homogeneously as in the unirradiated condition, the deformation is confined to planes or channels[11,12] that produce steps when they impinge on a grain boundary. Figure 5 illustrates the low-ductility grain boundary fracture that occurs in material irradiated below about 550°C to high neutron fluence and tensile or creep-rupture tested in the neighborhood of 550°C. The grain boundary surfaces are extremely smooth (even at 5000 to 10,000×), suggesting that no deformation occurred at or near the boundary. The fracture surface of the specimen irradiated to a fluence of 4.7×10^{22} neutrons/cm^2 was similar in appearance to that of the higher fluence sample, Fig, 5, and was almost entirely intergranular, with no evidence of the matrix deformation present in the lowest fluence sample. A small area similar in appearance to cleavage fracture was also present.

Auger spectroscopy results for the irradiated type 304 stainless steel samples are summarized in Table 3. When the samples irradiated to 4.7×10^{22} and 1×10^{23} neutrons/cm^2 were fractured, the system helium pressure increased. No increase occurred for the sample irradiated to 1.4×10^{22} neutrons/cm^2. From the observed pressure increase, system pumping speed, and volume, we estimate that 3.9×10^{11}, 1.6×10^{11}, and $<3.5 \times 10^{10}$ helium atoms were released from the high-, intermediate-, and low-fluence specimens, respectively. If the cross-sectional area of the sample is doubled to account for the surface irregularities, releases of about 0.08, 0.03, and <0.01 helium atom per atom of grain boundary are calculated, assuming 1.5×10^{15} grain boundary atoms/cm^2.

With the exception of the amount of helium released as the samples fractured, the composition of the grain boundary fracture surface did not seem to vary systematically with fluence. It is important to note, however, that the grain boundary fractures of the irradiated samples had higher nickel and iron concentrations and lower chromium concentrations than found on the ductile fracture surfaces of unirradiated samples fractured at the same temperature. This result is outside the uncertainty of the Auger analysis and does not appear to be attributable to test temperature, since increasing temperature generally caused both the chromium and nickel to increase in the unirradiated specimens. If the composition of the grain boundary fractures is compared to the bulk composition (instead of to a ductile fracture surface), then the iron was depleted, nickel enriched, and chromium approximately unchanged. As

---

[11]E. E. Bloom and J. O. Stiegler, "Effects of Fast Neutron Irradiation on the Tensile Properties of Austenitic Stainless Steels," pp. 768–72 in *Second International Conference on the Strength of Metals and Alloys, Conf. Proc.*, Vol. II, The American Society for Metals, Metals Park, Ohio, 1970.

[12]C. W. Hunter, R. L. Fish, and J. J. Holmes, "Channel Fracture in Irradiated EBR II Type 304 Stainless Steel," *Trans. Amer. Nucl. Soc.* 15: 254 (1972).

Table 3. Summary of Auger Spectroscopy Results for Type 304 Stainless Steel Irradiated at 370°C and Fractured at 550°C

Sample History and Type of Fracture	Atomic Fraction Present, Normalized to Fe + Cr + Ni = 1			Peak Height Ratios				Helium Release
	Fe	Cr	Ni	Si/Fe	P/Fe	S/Fe	Mn/Fe	
Unirradiated, ductile fracture	0.60	0.26	0.14	0.03	0.05	0.54	0.11	
1.4×10^{22} n/cm^2 (>0.1 MeV)								
Ductile fracture	0.62	0.27	0.11	0.03	0.05	0.40	0.06	No detectable helium release <1×10^{-9} torr-liters <0.01 He atoms / G.B. stie
Grain boundary fracture	0.67	0.19	0.14	0.02	0.15	0.33	0.09	
4.7×10^{22} n/cm^2 (>0.1 MeV)								
Grain boundary fracture	0.66	0.18	0.16	0.04	0.15	0.58	0.10	4.5×10^{-9} torr-liters 0.03 He atoms / G.B. site
1×10^{23} n/cm^2 (>0.1 MeV)								
Grain boundary fracture	0.64	0.20	0.17	0.03	0.11	0.17	0.05	1×10^{-8} torr-liters 0.08 He atoms / G.B. site

expected from the results on the unirradiated samples tested at 550 and 600°C, a significant amount of sulfur was present regardless of the type of fracture (ductile or grain boundary). The amount of phosphorus on the grain boundary fracture surfaces was 2 to 3 times that on the ductile fracture of the low-fluence sample or on the transgranular fracture of the unirradiated sample.

The composition as a function of depth from the grain boundary fracture surface at one location on a sample irradiated to 1.0×10^{23} neutrons/cm^2 (>0.1 MeV) was determined by sputtering at room temperature with argon ions. Results are plotted in Fig. 6. The concentration of the residual elements Si, P, S, and Mn decreased to levels below the detection limit of the apparatus within approximately the first five atomic layers from the boundary. Nickel, which was enriched at the boundary, and iron, which was depleted, also approached the bulk composition within the first few atomic layers. At the particular location at which the sputtering was conducted, the chromium concentration was higher than the average grain boundary value for the sample. During sputtering, the concentration decreased continuously, falling below the bulk composition after 40 min. The reason for this behavior is uncertain. A possible explanation is preferential sputtering of chromium atoms.

SUMMARY OF RESULTS AND DISCUSSION

Unirradiated Samples

Auger electron spectroscopy and scanning electron microscopy have been used to study the effects of irradiation on the fracture behavior of annealed type 304 stainless steel. Unirradiated samples tested in the range 25 to 600°C failed in a ductile transgranular mode. Auger analysis showed a monotonic increase in the concentration of sulfur on the fracture surface with increasing test temperature. At 550 and 600°C, small amounts of silicon and phosphorus were also found. The fact that the concentration of these elements increased with temperature suggests that segregation to the surface occurred as the samples fractured and/or were cooled from the test temperature. Segregation of solutes to interfaces such as free surfaces and grain boundaries is predicted from the Gibbs adsorption theorem. The mole fraction of solute at an interface, X_B^b, is approximately

$$X_B^b \simeq \frac{X_B \exp(Q/kT)}{1 + X_B \exp(Q/kT)} , \qquad (1)$$

where Q is the binding energy of solute to the interface and X_B is the concentration of solute in the matrix. For a given concentration of

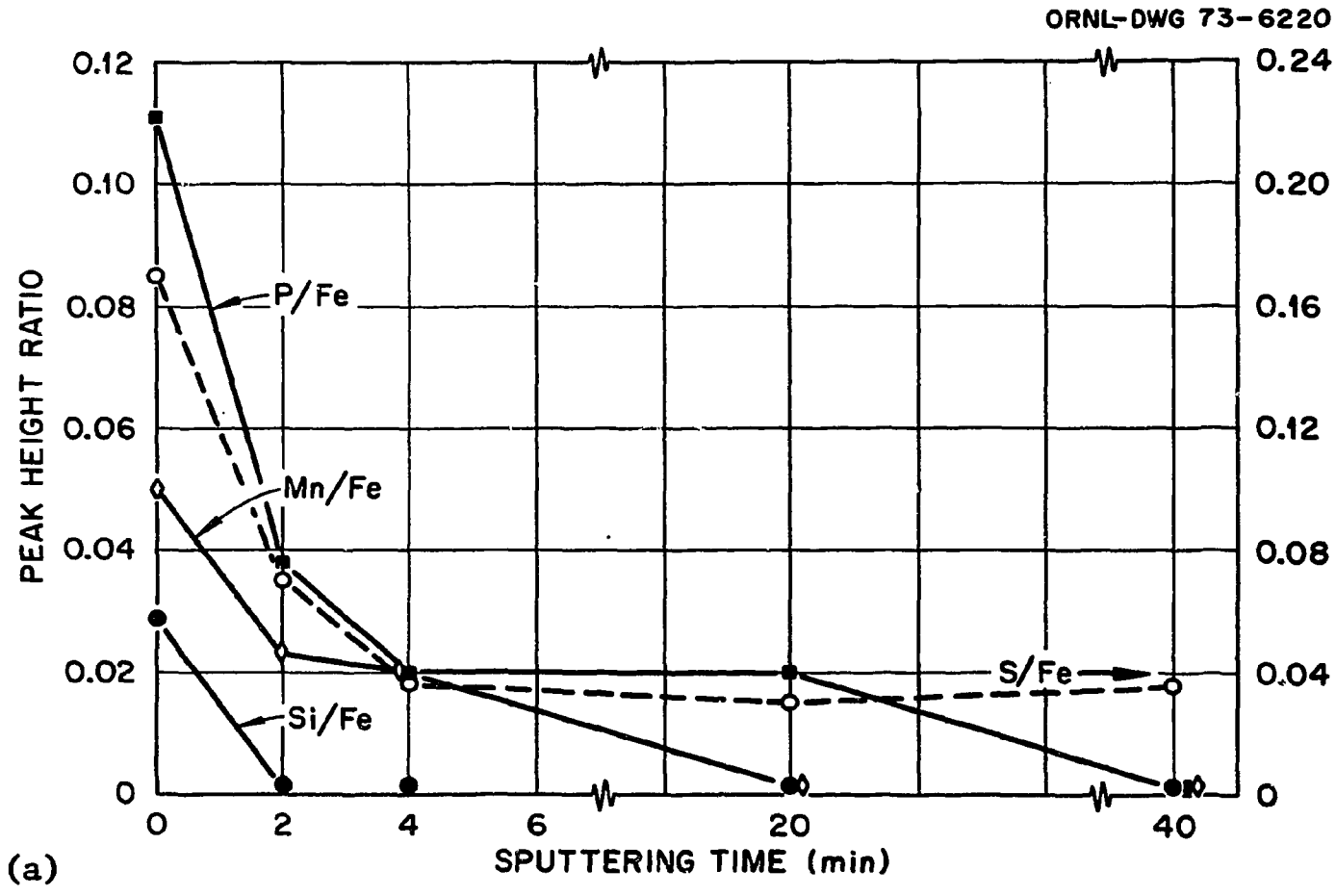

Fig. 6. Composition as a Function of Distance from the Grain Boundary in Type 304 Stainless Steel Irradiated at 370°C to 1×10^{23} neutrons/cm^2 (>0.1 MeV) and Fractured at about 550°C. One minute sputtering time equals about 1 atomic layer removed. (a) P, Si, Mn, and S. (b) Cr and Ni.

solute X_B the concentration at the boundary should decrease with increasing temperature. In the present results, the opposite trend was found. This is no doubt a reflection of the fact that equilibrium was not established because of the very short time at temperature. If we assume that equilibrium was approached for the sample fractured at 600°C, a value of Q can be calculated. From the Auger peak height ratios and relative sensitivity factors, we estimate that the mole fraction of sulfur in the fracture surface layers was 0.6. The alloy contained about 2.3×10^{-4} moles sulfur per mole of Fe, Cr, and Ni. The value of Q so obtained is 15,000 cal/mole. For comparison, Hondros,[13] using a zero creep technique, obtained a value of 16,000 cal/mole for grain boundary adsorption of phosphorus in bcc iron.

The present results show that in an austenitic stainless steel sulfur as well as other impurities segregate to free surfaces at elevated temperatures. The driving force for impurity segregation to a free surface (i.e., reduction in free energy) would be of the same sign as for segregation to grain boundaries, thus implying that grain boundary segregation of these elements would also occur. It is in the vicinity of one-half the absolute melting temperature that austenitic stainless steels (as well as nickel-base alloys) exhibit a tendency for intergranular fracture, particularly at low strain rates (i.e., lower than used in the present studies). The coincidence of these two phenomena suggests a possible casual relationship. Indeed, in the case of nickel and nickel-base alloys, the relationship between the sulfur concentration and high-temperature grain boundary fracture has been established.

Irradiated Samples

When tested at about 550°C, the irradiated samples failed in a predominately intergranular mode. Some areas of transgranular fracture were observed, particularly on the sample irradiated to the lowest neutron fluence (1.4×10^{22} neutrons/cm^2). The grain boundary fracture surfaces were very smooth and exhibited no evidence of ductile tearing or plastic deformation at or near the boundary. Only two structural features were observed on the fracture surfaces: sharp steps or ledges (Fig. 4) and a few widely spaced precipitate particles. In this material, tensile deformation often occurs in bands or channels rather than homogeneously throughout the matrix. The steps are thought to result from the intersection of these bands with the boundary.

Possibly the most important result of this investigation was the observed release of helium as the samples fractured, indicating that even at relatively low irradiation temperatures significant amounts of helium reach grain boundaries. Helium release was nearly proportional to the neutron fluence; about 0.08, 0.03, and <0.01 helium atoms per grain

---

[13] E. D. Hondros, "The Influence of Phosphorus in Dilute Solid Solution on the Absolute Surface and Grain Boundary Energies of Iron," *Proc. Roy. Soc. London*, A286: 479 (1965).

boundary site for fluences of 10, 4.7, and 1.4×10^{22} neutrons/cm^2 (>0.1 MeV), respectively. The average helium concentrations in these samples can be estimated from the empirical correlations of McElroy and Farrar.[14] The highest fluence sample contained about 28 ppm (atomic) helium. The amount of helium released during fracture was that produced within a volume extending about 3000 Å from either side of a grain boundary. The distribution of helium at the boundary is not known. Since bubbles were not visible by transmission electron microscopy, we conclude that the helium is either segregated to the boundary as a partial monolayer or is precipitated into very small bubbles probably less than about 20 Å in diameter. If precipitated as 20-Å-diam spherical bubbles, the average spacing would be about 100 Å, and about 4.5% of the boundary area would be occupied by bubbles. This seems to be a rather small fraction of boundary area to have such pronounced effects on properties and fracture behavior. Since the boundary probably consists of regions of "good fit" and regions of "bad fit" a uniform distribution of helium over the entire grain boundary area is unlikely. Rather, the helium may be concentrated in regions of "bad fit."

The grain boundary fracture surfaces of the irradiated samples were depleted in chromium and enriched in iron and nickel in comparison with ductile fractures produced at the same temperature. Since the grain boundary composition (with the exception of helium) did not vary with neutron fluence, it must be concluded that either (1) the irradiation-induced changes in grain boundary composition saturated at a fluence less than 1.4×10^{22} neutrons/cm^2 or (2) the observed grain boundary compositions (Fe, Cr, and Ni) are the approximate equilibrium boundary compositions. The second possibility seems less likely in view of the fact that both nickel and chromium tend to segregate to surfaces (as observed in the unirradiated ductile fractures at elevated temperatures), and thus one might expect both elements to segregate to grain boundaries rather than for chromium to be depleted and nickel enriched, as observed. Furthermore, segregation due to the boundary acting as a vacancy sink would be expected.

Tracer diffusion experiments by Perkins et al.[15,16] have measured diffusivities for Fe, Cr, and Ni in an Fe–17% Cr–12% Ni alloy of:

---

[14]W. N. McElroy and H. Farrar, "Helium Production in Stainless Steel and Its Constituents as Related to LMFBR Development Programs," p. 187 in *Radiation-Induced Voids in Metals* (Proc. Int. Conf., Albany, N.Y., June 9–11, 1971) ed. J. W. Corbett and L. C. Ianniello, AEC Symp. Ser. 26, CONF-710601 (April 1972).

[15]R. A. Perkins, "Tracer Diffusion of ^{63}Ni in Fe–17 wt % Cr–12 wt % Ni," *Met. Trans.* 4: 1665 (1973).

[16]R. A. Perkins, R. A. Padgett, Jr., and N. K. Tunali, "Tracer Diffusion of ^{59}Fe and ^{51}Cr in Fe–17 wt % Cr–12 wt % Ni Austenitic Alloy," *Metallurgical Transactions* (in press).

$$D_{Ni} = 8.8 \times 10^{-3} \exp(-60000/RT),$$
$$D_{Cr} = 0.13 \exp(-63100/RT), \text{ and} \qquad (2)$$
$$D_{Fe} = 0.37 \exp(-66800/RT) \text{ cm}^2/\text{sec}.$$

Anthony[6] has shown that in a binary alloy the ratio of the vacancy current to the impurity current (the impurity current is generated by the vacancy current to sinks) is

$$\frac{J_B}{J_V} = \frac{C_B D_B}{D_A + C_B D_B} \frac{\omega_1 - 13\omega_3/2}{\omega_1 + 7\omega_3/2} \quad , \qquad (3)$$

where:

J_B, J_V = solute and vacancy currents,

C_A, C_B = concentration of solvent and solute,

D_A, D_B = diffusivities of solvent and solute,

ω_1 = jump frequency from one nearest neighbor of a B atom to another,

ω_3 = jump frequency of a vacancy away from a B atom.

Further, the relative change in concentration $\Delta C_B/C_B$ during flow of vacancies to a grain boundary acting as a sink is

$$\Delta C_B/C_B = (J_B/J_V C_B)(\int_t J_V \, dt) \quad . \qquad (4)$$

The integral $(\int_t J_V \, dt)$ is the total number of vacancies flowing to the boundary in time t. At 370°C,

$$D_{Ni} = 4.8 \times 10^{-23} \text{ cm}^2/\text{sec},$$
$$D_{Cr} = 6.4 \times 10^{-23} \text{ cm}^2/\text{sec}, \text{ and} \qquad (5)$$
$$D_{Fe} = 1.0 \times 10^{-23} \text{ cm}^2/\text{sec},$$

from Eq. (2).

Since $D_{Cr} > D_{Ni} > D_{Fe}$, we would expect depletion of chromium and enrichment of iron at the boundary. Approximating the austenitic stainless steel as an Fe-Cr binary:

$$\frac{\Delta C_{Cr}}{C_{Cr}} = \frac{D_{Cr}}{D_{Fe} + C_{Cr}D_{Cr}} \left(\int_t J_V \, dt\right)\left(\frac{\omega_1 - 13\omega_3/2}{\omega_1 + 7\omega_3/2}\right) \quad . \tag{6}$$

Since the dislocation structure in the grain boundary denuded zone is similar to that in the matrix, we will assume that the number of vacancies and interstitials that either recombine or are lost to dislocations is the same as at large distances from the boundary. The highest fluence sample swelled about 8%, corresponding to approximately 6.6×10^{21} vacancies/cm^3 located in voids. If the denuded zone is 5×10^{-6} cm wide then $\int_t J_V \, dt = 17$ vacancies/grain boundary site. If $\omega_1 = \omega_3$, then $J_{Cr}/J_V = -0.65$ and $\Delta C_{Cr}/C_{Cr} = -62$. Thus significant depletion of chromium (and nickel by virtue of the fact that $D_{Ni} > D_{Fe}$) and enrichment of iron should have occurred in the grain boundary regions. There are several possible reasons why extensive segregation was not observed. In the development of Eq. (3) impurity flow resulting from a gradient in the impurity concentration in the absence of a gradient in the free vacancy concentration was neglected. As pointed out by Anthony[6] this will tend to buffer any buildup of a solute gradient. A second possible factor that would tend to reduce segregation due to the vacancy current would be the diffusion of irradiation-produced self-interstitials into the boundary. However, this would be important only if the self-interstitials diffuse relatively long distances by an interstitial mechanism. If, however, diffusion occurs by an interstitialcy or crowdion mechanism then a given self-interstitial atom will move only a short distance and thus have no significant influence on concentration gradients. Thirdly, as we have already seen, the concentrations of chromium and nickel on the fracture surface of an unirradiated sample tend to increase with test temperature (see Table 2). This would tend to decrease the amount of irradiation-induced depletion observed in the present experiment.

Sulfur and phosphorus were found on the grain boundary fracture surfaces. The fact that sulfur was present is not surprising in view of the fact that it was observed to segregate to surfaces during and/or after fracture at elevated temperatures. Phosphorus was also present on the fracture areas of grain boundaries. It appears that this segregation existed before test, since it was more pronounced in areas of grain boundary fracture on the same sample and the concentrations were generally higher than found on unirradiated ductile fracture surfaces. From the present results, it cannot be established whether the segregation of phosphorus is an equilibrium phenomenon or a result of the boundary acting as a vacancy sink during irradiation. Since the amount present at the boundaries did not change with fluence, we conclude that the segregation is an equilibrium condition or that it occurs early in the irradiation and then saturates at higher fluences.